EUROFUSION WPHCD-PR(16) 16623

G Cartry et al.

Alternative solutions to caesium in negative-ion sources: a study of diamond as negative-ion enhancer material in H2/D2 plasmas

Preprint of Paper to be submitted for publication in
New Journal of Physics

This work has been carried out within the framework of the EUROfusion Consortium and has received funding from the Euratom research and training programme 2014-2018 under grant agreement No 633053. The views and opinions expressed herein do not necessarily reflect those of the European Commission.

This document is intended for publication in the open literature. It is made available on the clear understanding that it may not be further circulated and extracts or references may not be published prior to publication of the original when applicable, or without the consent of the Publications Officer, EUROfusion Programme Management Unit, Culham Science Centre, Abingdon, Oxon, OX14 3DB, UK or e-mail Publications.Officer@euro-fusion.org

Enquiries about Copyright and reproduction should be addressed to the Publications Officer, EUROfusion Programme Management Unit, Culham Science Centre, Abingdon, Oxon, OX14 3DB, UK or e-mail Publications.Officer@euro-fusion.org

The contents of this preprint and all other EUROfusion Preprints, Reports and Conference Papers are available to view online free at http://www.euro-fusionscipub.org. This site has full search facilities and e-mail alert options. In the JET specific papers the diagrams contained within the PDFs on this site are hyperlinked

Alternative solutions to caesium in negative-ion sources: a study of diamond as negative-ion enhancer material in H_2/D_2 plasmas

Gilles Cartry, Dmitry Kogut[1], Kostiantyn Achkasov[1], Jean-Marc Layet[1], Thomas Farley[2], Alix Gicquel[3], Jocelyn Achard[3], Ovidiu Brinza[3], Thomas Bieber[3], Hocine Khemliche[4], Philippe Roncin[4], Alain Simonin[5]

[1] Aix-Marseille Univ, CNRS, PIIM, UMR 7345, 13013 Marseille, France
[2] CCFE, Culham Science Centre, Abingdon, Oxon, OX14 3DB, UK and Department of Electrical Engineering and Electronics, University of Liverpool, Brownlow Hill, Liverpool, L69 3GJ, UK
[3] LSPM, CNRS-UPR 3407 Université Paris 13, 99 Avenue J. B. Clément, F-93430 Villetaneuse
[4] Institut des Sciences Moléculaires d'Orsay (ISMO), CNRS, Univ. Paris-Sud, Université Paris-Saclay, F-91405 Orsay, France
[5]CEA, IRFM, F-13108 Saint-Paul-lez-Durance, France

Abstract

Modern and efficient H^-/D^- negative-ion sources use caesium injection in the H_2/D_2 plasma to enhance production of negative-ions at the extraction grid. This solution is up to date the only known way to reach the negative-ion currents required for fusion or accelerator applications. However, caesium injection complicates the long term operation of these sources and alternative solutions would be highly valuable. In this paper we discuss briefly alternative materials that could be used to enhance surface production of negative-ions in low-pressure, low-temperature H_2/D_2 plasmas. We then show some results obtained on diamond layers used as negative-ion enhancer materials.

Introduction

Negative-ion production on surfaces in low-pressure plasmas rely on two distinct mechanisms. Depending on where the ions are formed, one distinguishes volume production[1,2,3,4,5] associated with dissociative attachment of electrons on molecules while surface production is associated with the capture of one or two electrons by neutral or ions impinging the surface. Depending on the targeted application, surface or volume production can be the most favored process. Hydrogen negative-ion sources for fusion[6,7], for high energy linear particle accelerators[8,9,10] or neutron generation[11], as well as sources for Tandem accelerators or for accelerator based mass spectrometry[12,13] use the principle of enhanced surface production by injection of caesium. Negative-oxygen-ion sources for Secondary Ion Mass Spectrometry (SIMS) operate by volume production. Space propulsion with plasma thrusters (LPP-ICARE) [14,15,16], or plasma etching for microelectronics[17,18,19,20,21,22], might use in the future negative-ion sources that are expected to rely on volume production but may also benefit from surface production.

The present work deals with negative-ions for fusion applications in the context of the international projects ITER and DEMO aiming at controlling nuclear fusion to produce energy. In tokamaks (nuclear fusion reactors), a plasma composed of deuterium and tritium is magnetically confined and heated to very high temperatures around $1.5 \cdot 10^8$ K to overcome the repulsion between deuterium and tritium nuclei and achieve fusion. The ITER device is a research tool, aiming at studying magnetically-confined nuclear-fusion, and providing technological solutions for its successor, the DEMO project. DEMO will be the first nuclear-fusion power-plant prototype producing energy, it is targeting~1 GW of electrical power coupled to the grid[23,24]. In ITER and DEMO devices, the heating of the plasma will be mainly obtained thanks to the Neutral Beam Injector devices (NBI). NBI are key components in achieving high fusion energetic-performances. The NBI inject into the tokamak 1 MeV deuterium (D) neutral-beams providing heating and current drive of the fusion plasma. At such high velocities, much larger than the typical electron velocity, the probability of electron capture from D^+ ions is too low so that production of D° relies on electron detachment from high-intensity D^- beams. D^- negative-ions are produced in a low-pressure plasma source and subsequently extracted and accelerated.

The ITER negative ion source, currently under development in Germany at IPP Garching[25,7] , operates with a high-density low–pressure inductively coupled plasma. Extracted D^- current density of 200 A/m^2, over a large surface of 1.2 m^2, with 5-10% uniformity and low co-extracted electron-current (below one electron per negative ion), during long operation period (3600 s) is targeted. To reach such a high D^- negative-ion current, the only up-to-date scientific solution is the use of caesium. Deuterium negative-ions are created at the extraction region by backscattering of positive ions or neutrals on the plasma grid. Deposition of caesium on the grid lowers the material work function and allows for high electron-capture efficiency by incident particles and thus, high negative ion yields. Studies conducted at IPP Garching show that the ITER negative-ion source can reach the required high current densities. However, drawbacks to the use of caesium have been identified. First, the caesium is continuously injected in the source and its consumption is huge, in the range ~5-10 µg/s[26]. Second, caesium diffusion and pollution of the accelerator stage might cause parasitic beams and/or voltage breakdowns and imply a regular and restrictive maintenance in a nuclear environment. Finally, long-term operation stability with caesium appears to be a technological bottleneck requiring a strict, long, difficult and controlled conditioning of the negative-ion source. These issues complicate the operation of the ITER-NBI and pushes towards a strong reduction of caesium consumption or even the development of caesium-free negative-ion sources for DEMO. The aim of the present work is to investigate alternative materials to caesium-coated metals for surface production of high negative-ion yields in low pressure H_2 or D_2 plasmas.

Surface production of negative-ions in low-pressure caesium-free plasmas is of interest from a fundamental point of view since it is a part of the global plasma dynamics and might influence it strongly. However, few papers [27,28] have been dedicated to this subject, and most of them are related to the process of thin film deposition by magnetron plasma sputtering [29,30,31,32,33,34,35,36,37,38,39,40,41,42,43,44,45,46,47,] In such a process, sputtered negative-ions might influence the properties of the deposited layer. Most of these studies concern O^- negative ions. As the negative-ion surface production is seen as a drawback, because of possible damage on deposited-layers caused by fast negative-ions, there is no study of negative-ion yield optimization. Therefore,

in order to find alternative solutions to caesium for fusion applications, there is a need for fundamental studies on negative-ion surface production in low-pressure H_2 and D_2 caesium-free plasmas. In this context we are studying H^-/D^- surface production on diamond surfaces. The aim is to understand and optimize surface production. The paper is organized in four parts. In the first part the basic principles of negative-ion surface production as well as possible negative-ion enhancer materials are briefly presented. In the second part the choice of diamond as a negative-ion enhancer material is justified. The experimental methods are detailed in the third part. The last part is devoted to the study of negative-ion surface production on diamond, it summarizes previous results on diamond layers and recent measurements showing the performances of diamond as a negative-ion enhancer material. Results for intrinsic or boron-doped microcrystalline, nanocrystalline and single crystal layers will be presented and compared to graphite (Highly Oriented Pyrolitic Graphite, HOPG) taken here as a reference material.

Negative-ion surface production

Basic mechanisms of negative ion formation at surfaces

There is an extensive literature on negative-ion surface-production in well-controlled beam-experiments at grazing incidence, for a large variety of incident energy and ion particle type and a large variety of surfaces, see for instance references 48, 49, 50, 51, 52, 53, 54, 55, 56, 57, 58 and references therein. Negative-ion surface production under quasi-normal incidence has been less studied. From these studies, the fundamental mechanisms of negative-ion surface-production on metallic surfaces have been established for many years[53,59,60].

Most often beam experiments use positive ions as projectiles, but these are assumed to undergo rapid neutralization on the incoming part of the trajectory leading to so called memory loss effect. Negative-ion formation consists then in the capture of an electron by a neutral projectile whatever the incoming particle is (atom or ion). Electron transfer from or to a metal surface (see figure 1) is mainly governed by two basic parameters. One is the difference in energy (mismatch) between the affinity level of the negative ion and the Fermi level or the valence band where electrons are to be captured. The second parameter is the coupling, given by the wave function overlap, between these levels which governs the exchange rate. Both ingredients depend on the distance to the surface and the projectile parallel velocity. On approaching the surface the affinity level is **smoothly** downshifted by the image potential while electron tunneling transfer rates from the surface to the projectile affinity-level or backward increases **quasi-exponentially**. At some distance, rates are so large that memory of the initial charge state is lost. Close to the surface the projectile equilibrium charge state is a negative ion. However, when leaving the surface, the affinity level rises back and faces empty states in the conduction band so that the electron will eventually return to the surface, **unless** the rates have sufficiently decreased or the available time is too short, i.e. the velocity too large. This leads to the concept of freezing distance[61] describing the velocity dependent critical distance where electron transfer rates become negligible; the outgoing negative ion fraction reflecting only the local capture and loss rates.

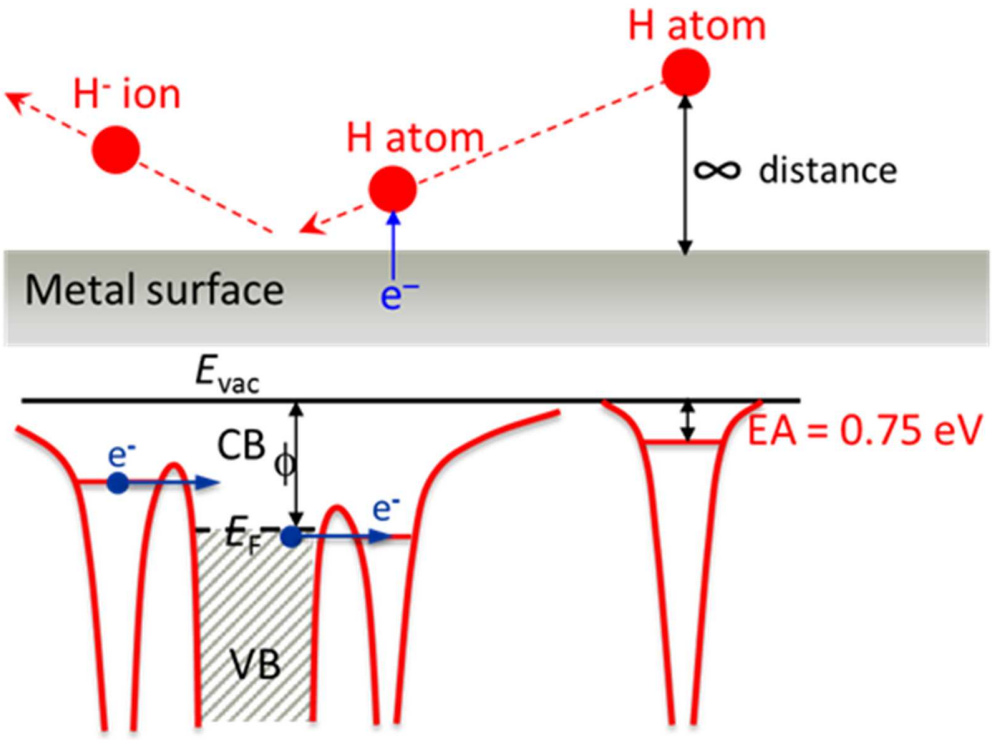

Figure 1: sketch of the mechanism of electron capture by an incoming hydrogen atom on a metal surface (on top spatial representation, on bottom energetic representation)

When depositing caesium on the surface, the material work-function is lowered reducing the energy barrier so that the freezing distance is now placed in the region where negative ions dominate. Usual metal work functions are on the order of 5 eV while a thick caesium deposit on the metal will lead to a work function of 2.1 eV (the work function of caesium itself)[62]. The surface work-function can be further reduced in the range of 1.5 eV if only ~half monolayer of caesium is deposited on the surface[63,64]. However, due to the complexity of a real negative-ion source, there is little chance to obtain such a control of the caesium coverage[65,66,67]. More interesting here, if the work-function is low enough, the freezing distance will remain in the favorable region even for low velocity projectiles allowing atoms with ~eV energies to contribute to the negative ion production. This explains the success of the giant negative-ion source for ITER where the atomic flux, which largely exceeds the ionic flux, is able to contribute to the negative-ion surface production.

For insulators or semi-conductors, electrons are localized and more deeply bound resulting in much lower electron capture rates so that even full neutralization of positive ions is not granted. Still, a general mechanism explaining significant negative ion formation has been identified recently[68]. In addition to the image potential effect, the downshift of the affinity level is further amplified by the Coulomb interaction between the negative ion and the localized hole on the outgoing part of the trajectory. Furthermore, the electron loss back to the surface can be reduced or suppressed because no empty states are present in the band gap to recapture the electrons on the way out. Such models have explained that on LiF(100) surface known to have one of the largest work function , yields

of 10% H^- have been observed at grazing incidence[69,70], more than one order of magnitude larger than from an Al surface[48].

There are even few examples where negative ion formation directly from the positive ion, i.e. simultaneous capture of two electrons[50,51] was found to be more likely than single electron capture from the neutral atom. This has been explained with the above quasi molecular model including coulombic attraction and by the fact the negative energy defect of the first event can be compensated by the positive one of the second event provided that they take place simultaneously. This mechanism is potentially interesting for negative-ion surface production but will not be discussed further in this paper.

Caesium and its alternatives

The story of plasma-based negative-ion sources started in 1971 with the discovery of the caesium effect by the Russian scientists V Dudnikov and Y Belchenko[71] (see also review papers 72, 73). Up to 1989, two kinds of negative-ion sources were developed, namely the volume sources and the surface-plasma sources (SPS), where negative ions were created on a negatively-biased cathode facing the extractor. The cathode was usually made of low work-function materials and it has been shown that barium could be as efficient as caesium[74,75,76] since the optimum caesium coverage of half a mono-layer cannot be realistically obtained in a real negative-ion source. Furthermore, barium was not presenting major conditioning issues and its surface was simply prepared by argon sputtering[77]. In 1989, Leung[78] demonstrated that the injection of caesium vapor in volume sources largely increased the extracted negative-ion current. This new type of sources was called hybrid-sources. It took many years of research on Cs-seeded sources before understanding that the efficiency of the hybrid sources is mainly due to the creation of negative-ions on the plasma grid, very close to the extractor[79]. The observed effect is *a priori* not inherent to caesium and could probably be obtained by using other material for the plasma grid. However, studies were strongly focused on caesium during many years and alternative solutions have not been investigated deeply. Therefore, revisiting the efficiency of low-work function materials, other than caesium, in the light of modern negative-ion source developments would be interesting. Such studies have recently started at IPP Garching[80]. Another solution to reduce the drawback of caesium would be to limit its injection in the source. Some recent work[81,82] have shown than caesium-implanted molybdenum can present high negative-ion yield and could be an interesting solution for fusion. Several arguments go into the favor of this solution: i) implanted caesium would act as a reservoir for the surface; ii) less than one monolayer of caesium is required to optimize surface production, and this can be achieved by caesium implantation; iii) there is a high chance that the caesium coverage of the extraction grid in actual negative-ion source is not huge even when injecting massive amounts of caesium since the grid temperature is quite high 150-200 °C[67,7]; iv) the grid could be re-implanted *in-situ* when the caesium reservoir inside the material is depleted. However, further studies are required to check the capability of this technique and verify that large enough caesium surface concentration (few tens of percent) can be reached together with low contamination.

As explained before, insulating materials, in particular large band gap materials, could be interesting to enhance negative-ion surface production in plasmas. In the ITER negative-ion source, the plasma grid on which extracted negative-ions are formed is biased between the floating and the

plasma potential[83]. Therefore using an insulating material at floating potential as plasma grid would not be *a priori* an issue. Among insulators, we have selected diamond for many reasons. First of all carbon materials appear to be among the best candidates as negative-ion enhancer materials in caesium free plasmas. A negative-ion yield of 10% on graphite (HOPG, Highly Oriented Pyrolytic Graphite) has been obtained at ISMO[84], and slightly lower yields have been reported on diamond-like carbon (DLC)[85] (yield is defined as the ratio between the negative-ion flux leaving the surface and the positive ion flux impinging on the surface). DLC material has even been chosen as a converter material for the low-energy heliospheric neutral atom sensor (neutral to negative-ion converter) installed on the IBEX satellite launched in 2008. Furthermore, in reference 86, the yield measured on diamond was twice that measured on graphite, showing that diamond is a promising negative-ion enhancer material. Secondly, we have shown an increase of negative-ion yield on diamond by a factor 5 compared to graphite when heating to ~ 400°C the diamond surface exposed to the plasma[87]. Thirdly, diamond can be produced in several forms such as single crystals with usually small area up to 1 cm^2 and a few mm in thickness[88], polycrystalline films with thickness of 1 to 100 µm, with a surface area of up to 5000 cm^2 [88,89], nanocrystalline films with grain size down to 5 nm[90,91,92]… Tuning of electronic properties, for instance by varying the band gap can be obtained by deposition of intrinsic, lightly or highly doped with boron (p-doped), nitrogen, or phosphorous (n-doped) diamond films. In addition, diamond surface properties depend on the surface crystallographic face as well as on the termination of the dangling bonds which can be oxygen or hydrogen terminated. Finally, and it is the most interesting property of diamond, hydrogenated diamond layers may exhibit negative electron affinity i.e. the minimum of the conduction band is above the vacuum level[93,94] so that electrons are free to leave the surface. Here, the anticipated advantage would be that the limited bandgap implies that the valence band is close to the vacuum level favoring electron capture while still limiting the electron loss by preventing the return to the surface. Also, if some electrons are promoted in the conduction band by the UV radiations of the plasma, they could be easily captured. The negative-electron affinity of diamond probably explains the excellent field emission capabilities[95] of diamond as well as the observation of very high secondary electron emission yield; up to 80 emitted electrons upon single electron bombardment on a (100) single-crystal with hydrogenated or cesiated surface[96]. Due to the ability of diamond and hydrogenated-diamond to emit high flux of electrons, diamond is expected to be efficient for producing negative-ions. This last hypothesis is empirical since the basic mechanisms of surface ionization are different from the mechanism involved in the field or secondary electron emission. Nevertheless, a good correlation between ion-induced secondary emission yield and O^- negative-ion yields has been observed for several materials in a magnetron plasma[30].

Experimental method

Surface production measurements are performed in the diffusion chamber of a plasma reactor. The plasma is generated at 2 Pa, either by capacitive coupling from an external antenna using a 20 W 13.56 MHz generator, or at 1 Pa by an Electron Cyclotron Resonance heating driven by a 60W 2.45 GHz generator. The plasma density, as measured by Langmuir probe, is $ne = 2 \cdot 10^{13}$ m^{-3} and the electron temperature is Te = 3.5 eV, giving an ion flux to the sample of the order of 10^{17} $m^{-2}s^{-}$

[1] in RF mode. In case of ECR plasma, ne = $2.5 \cdot 10^{15}$ m^{-3}, Te = 1.0 eV and the ion flux to the sample is ~7 10^{18} $m^{-2}s^{-1}$. The sample holder lies in the center of the diffusion chamber, facing a Hiden EQP 300 mass spectrometer equipped with an energy filter. Details on experiments can be found elsewhere[97,98]. Figure 2 shows a simple sketch of the experimental arrangement. The sample is negatively biased with respect to the plasma potential so that Negative-Ions (NI) emitted from the surface are accelerated towards the plasma and self-extracted from the plasma to the mass spectrometer where they are detected according to their energy. The measurement gives the Negative-Ion Energy Distribution Function (NIEDF). There are two major advantages to this experimental arrangement. First, samples can be simply changed thanks to a fast load lock system, and this would not be possible if one would study materials deposited on an extraction grid. Second, the physics of the ion extraction is quite simple and can be easily accounted for to focus on surface production rather than extraction issues. The main disadvantage is the requirement of a negative bias to get the self-extraction effect. Positive ions bombard the sample and create defects. The pristine material is modified and its surface state has to be characterized afterwards.

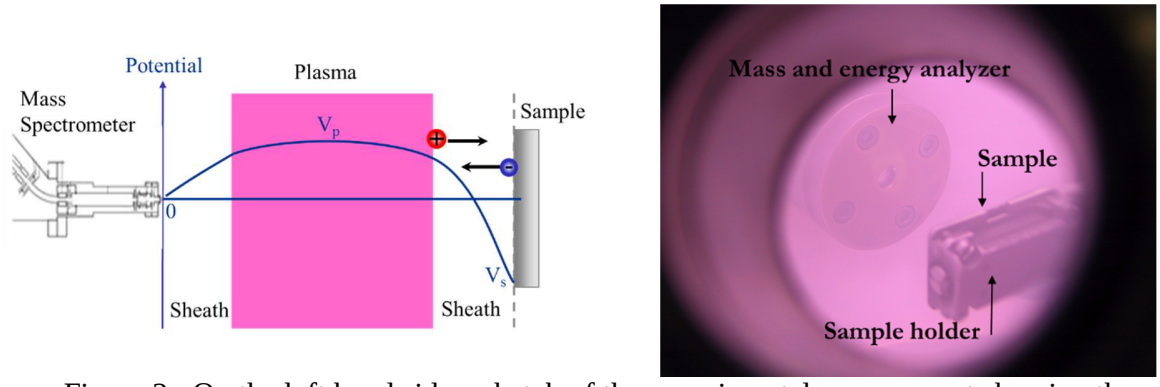

Figure 2: On the left hand side a sketch of the experimental arrangement showing the electrical potential profile between the sample holder and the mass spectrometer. On the right side a picture showing the sample holder facing the mass spectrometer.

In beam experiments, most of the information on the surface production mechanisms is concentrated in scattering differential cross section of the products associated with well-defined momentum of the primary projectile. In plasma the measurement is reduced to the Energy and Angle Distribution Function of the emitted Negative-Ions (NIEADF) which is already difficult to obtain since the negative-ions have to be extracted before being measured. The measured Negative-Ion Energy Distribution Function NIEDF is strongly different from the NIEDF of emitted ions because of the presence of electric fields in the sheaths that modify trajectories. Simulations are needed to take into account these effects. In order to determine the Negative-Ion Energy and Angle Distribution Function (NIEADF), we first chose *a priori* the NIEADF, then calculate ion trajectories inside the sheath, and finally produce NIEDF restricted to the ions reaching the mass spectrometer within its acceptance angle. The computed NIEDF are compared to the experimental ones. The *a priori* choice made for the NIEADF is validated when a good agreement between the computed and the measured NIEDF is obtained as displayed in figure 3 and ref (97,98). This method requires an accurate guess of the solution. To generate angular and velocity distributions, we used the SRIM[99] software to compute the contributions from sputtered and backscattered

particles leaving the surface [28,100,101,102]. As SRIM does not take into account surface ionization, attributing the SRIM distribution functions to the emitted negative-ions is a strong assumption, implicitly stating that the surface ionization probability has no dependence on the energy and angle of the outgoing particle. In the present context where several averaging occur in the simulation, this has been found to be an acceptable assumption for carbon materials[97,98]. The input for the SRIM computations were the positive ion distribution functions, as measured by the mass spectrometer and the surface parameters namely the hydrogen surface coverage, the hydrogen surface binding energy… Here, we benefited from intensive studies of carbon material as a plasma facing component in tokamaks. SRIM computations for hydrogenated carbon layers have been largely validated. But this cannot, *a priori*, be generalized to any material. We have therefore developed a second method to derive the NIEADF where NIEDF are measured for several tilt angles (named hereafter α) of the sample normal with respect to the mass spectrometer axis. When rotating the sample, ions emitted at higher angles and/or higher energies can be measured. By using NIEDF measured at all tilt angles (figure 4a), an inverse calculation can be performed to determine the NIEADF without any *a priori* assumption[103]. This distribution function is presented in a polar plot on figure 4b. There is an overall good agreement [103] between both methods. The second method can however be generalized to any kind of material and any negative-ion type. The results presented in figure 3 and 4 concern HOPG material but identical results are obtained with diamond layers.

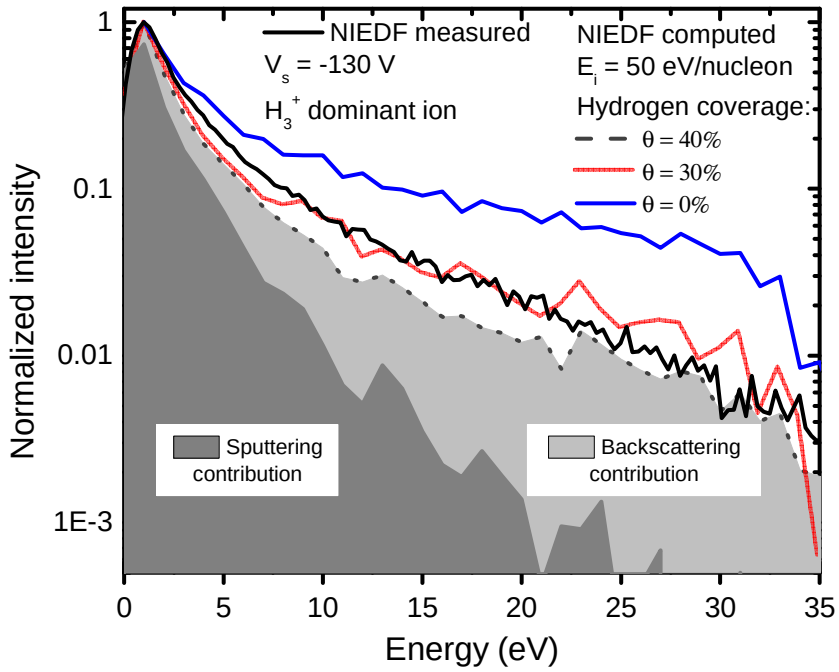

Figure 3: Comparison between calculated NIEDF at mass spectrometer for HOPG in hydrogen plasmas for different values of hydrogen surface coverage θ. The contributions of sputtering and backscattering are shown for θ = 40%. The model compares well to the experiment for θ = 30%

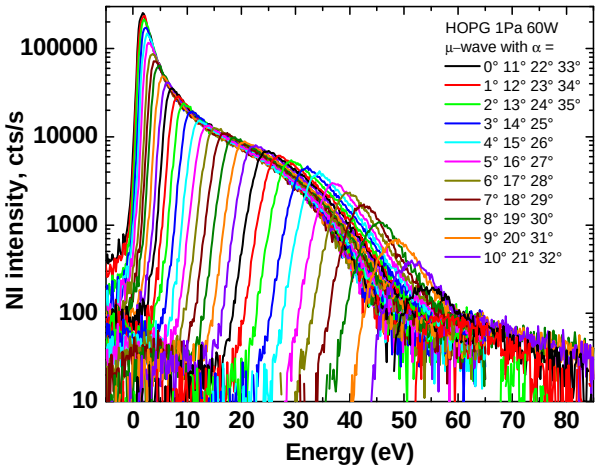

Figure 4a: Experimentally measured mass spectrometer NIEDF for different tilts of HOPG sample: from α = 0° to 35°, with a step of 1°. ECR plasma 1 Pa, 60 W

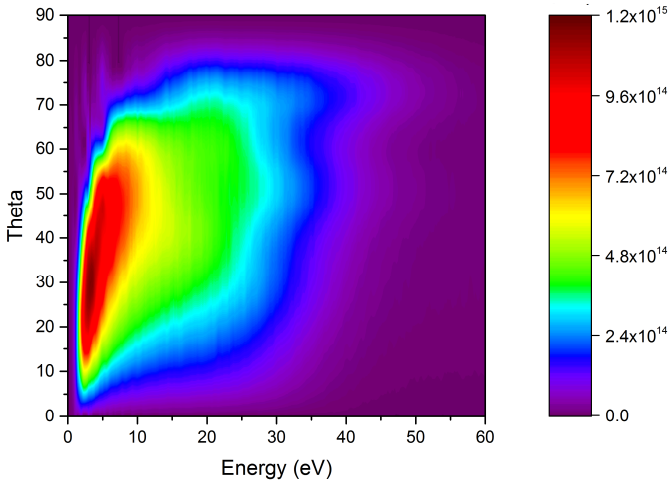

Figure 4b: NIEADF reconstructed from the experiment of figure 4a. The color coded intensity map indicate the number of NI emitted from the surface at an angle θ and with an energy E.

These calculations provide the hydrogen surface coverage, more precisely the coverage of hydrogen participating to the sputtering process leading to negative-ion formation. For both HOPG and diamond layers it was found to be of the order of 30% at room temperature, in RF and ECR plasmas, with a sample bias of -130 V. Furthermore, the calculations showed that negative ions originate from a disc of diameter < 2 mm centered on the 8 mm diameter sample under the chosen experimental condition. The clamp and the sample holder surfaces therefore do not contribute to the total yield of negative ions. The calculations also show that the sputtered negative ions are emitted at lower angle and energy than backscattered ions and hence those are preferentially detected when the sample surface is normal to the mass spectrometer axis ($\alpha = 0°$). While 95% of ions are emitted by the backscattering process, about 40% of ions being detected when $\alpha = 0°$ have been created by the sputtering process. Moreover, only a few percent of the emitted negative-ions are detected, for instance 1.6% for the condition at 2 Pa and 20 W RF power. Rotating the sample is therefore crucial to collect information representing the total negative-ions distribution. When comparing two materials on the sole basis of the distribution recorded at $\alpha = 0°$, one must ensure that their angular emission are identical. This verification has been made for all measurements shown in this paper. The models also demonstrate that the shapes of the measured energy distribution functions are mainly determined by the proportion of sputtered and backscattered negative ions detected as demonstrated on figure 3. When tilting the sample, the main peak, originating from sputtered negative-ions, disappear[98] and negative-ions originating from backscattering mechanism are probed. Finally, the models show that the measured NIEDFs (figure 3 and 4a) are very different from the distribution functions of the particles emitted by the surface[98].

This difference is due to the low number of ions collected by the mass spectrometer at a given tilt angle of the sample.

Diamond as a negative-ion enhancer material: results and discussion

Figure 5 compares relative negative-ion yields obtained on graphite (HOPG) and diamond materials in D_2 RF plasma (2 Pa, 20 W, surface bias V_s = -130 V) for different surface temperatures. The NI yield is usually defined as the ratio between the negative-ion flux leaving the surface and the positive ion flux impinging on the surface. Under the present experimental conditions the positive-ion flux is constant. Therefore, the relative NI yield is simply defined as the measured total flux (counts per second) of negative-ions (i.e. the area below the measured NIEDF). It has been checked that the angular emission behavior of all the layers studied is identical, hence a comparison of yields measured at $\alpha = 0°$ is enough. As it was already demonstrated in H_2 plasma, the negative-ion yield on diamond exhibits a maximum around 400–500°C while the yield on graphite is continuously decreasing. Two diamond layers are presented here: i) MCBDD, micro-crystalline boron-doped diamond (SEM pictures and information can be found in 104, the doping level is estimated to be 1.5×10^{21} cm^{-3}); ii) MCD, micro-crystalline diamond (basically it is a sample very similar to MCBDD but without boron doping, see SEM picture on figure 6 where a strongly multitwinned polycrystalline diamond film is shown. More materials are compared in 105. It can be observed that boron doping, which is a p-doping, does not seem to influence neither the negative-ion yield or the global behavior of the yield with temperature. However, one can notice that no data points have been obtained for MCD at temperature lower than 300°C. The reason is that the un-doped MCD layer turned out to be insulating at lower temperature when exposed to H_2 plasma (2 Pa, 20W RF). As the self-extraction method requires a negative DC bias of the sample, it was not possible to undergo any measurement on MCD from room temperature to 300°C. As a conclusion on the role of boron doping, we could say that it simplifies the present study by giving a good sample conductivity but does not seem to influence the NI yield.

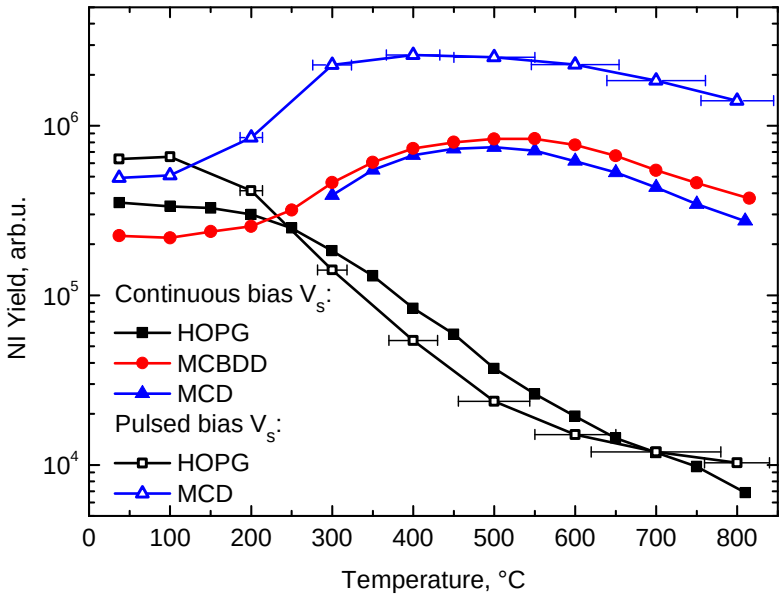

Figure 5: NI yield dependence on the surface temperature for HOPG, MCBDD and MCD for constant bias (solid symbols) and pulsed bias (empty symbols). Plasma parameters: 2.0 Pa of D_2 RF plasma, 20 W. Pulsed bias parameters: Tpulse = 15 µs, Tacq = 10 µs, f = 10 kHz, Vs = –130 V.

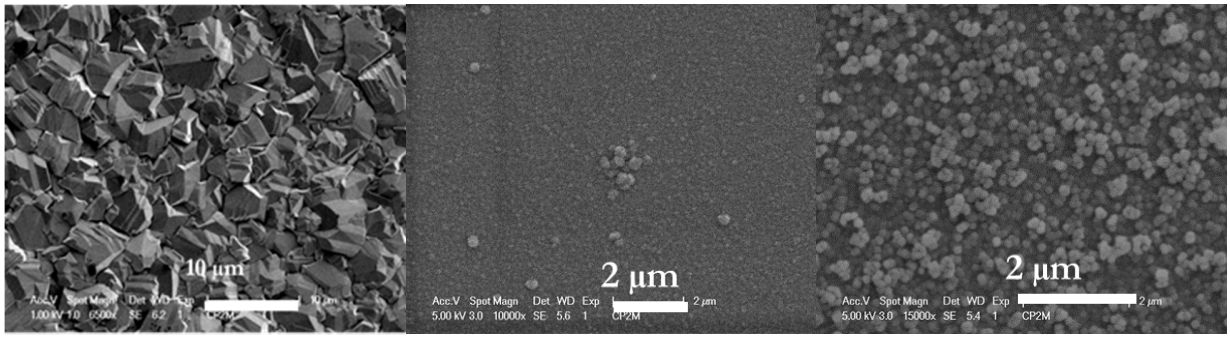

Figure 6: SEM picture of MCD material (micro-crystalline diamond), NCD 1% and NCD 5% deposited on Si at LSPM laboratory. Thickness is from 2 to 10 µm for MCD and around 200 nm for NCD depending on the sample used.

The increase of the negative-ion yield with surface temperature is still under study. However, surface analyses, in particular Raman spectroscopy, have provided insight into the understanding of this behavior[87,104]. At room temperature, the ion bombardment creates some defects on the material and lead to its hydrogenation. The positive ion energy in figure 5 is around 135 V (plasma potential minus surface bias). As H_3^+ is dominating the positive ion flux, the energy per nucleon of positive ions impinging the surface is around 45 eV. The impacts lead to the creation of a

hydrogenated carbon layer having a certain hybridization ratio sp^2/sp^3, most probably higher for graphite than diamond. Raman spectra reveal that sp^2 phases on the MCBDD surface disappear with the temperature increase. Defects/non diamond phases produced by plasma exposure are annealed and etched away by the plasma at high temperature. Enhanced sp^2 phases etching at high temperature has indeed already been observed[106,107]. Therefore when increasing the temperature, the diamond surface is reconstructed and the surface state is probably closer to the pristine material than at room temperature. At 800°C, the diamond layer almost recovers its original Raman signature. From the modelling presented previously we learn that up to the maximum in negative-ion yield, the hydrogen surface coverage is slightly increasing (from 30 to 35%) while it decreases after the maximum. H-free (100) diamond surface has shown positive electron-affinity contrary to hydrogenated (100) surface which presents negative electron-affinity[93]. Therefore we can assume that upon heating under plasma exposure from room temperature to 400-500°C the diamond layer recovers its electronic properties and among them, its negative-electron affinity. When further increasing the temperature, hydrogen atoms desorb and the negative-electron affinity is lost. Concerning graphite, Raman measurements show that its surface is reconstructed upon temperature increase, and the modelling demonstrates that the hydrogen coverage is going down to zero. However, the decrease of the negative-ion yield is much bigger than the one expected from the complete suppression of the sputtering mechanism. Therefore, one can conclude that sp^2 hybridization is not favorable for negative-ion surface creation under our experimental conditions (i.e. under high energy ion impacts at normal incidence). This is confirmed by the time evolution of negative-ion yield in D_2 plasma presented in figure 7a. Both materials have been heated to 500°C under vacuum prior to plasma exposure in order to remove impurity contamination. Once the plasma is started, some defects are created on the surface (sp^3 defects for HOPG, sp^2 defects for Diamond) and hydrogen is implanted. One can observe that the negative-ion yield is increasing for HOPG (the creation of sp^3 defects favors negative-ion creation), while it is strongly decreasing for MCBDD (the creation of sp^2 defects is not favorable). Figure 7b shows a similar measurement in deuterium plasma. The empty symbols represent the negative-ion yield from the first series of measurement on a virgin MCBDD sample. One can observe a major NI yield decrease during the first 5 minutes (see black empty symbols) probably connected to the degradation of the sample surface. When the surface state is stabilized, the negative-ion yield stays constant. Then, the heating of the sample was performed in plasma during ~ 1 min at surface bias V_s = -130 V still applied. The red empty symbols show the increase of negative-ion yield after the heating to 400°C which also happens within 5 minutes. The negative-ion production becomes more efficient and the yield rises a bit below the initial level. It can be assumed that the surface state has partially recovered from the defects induced by the plasma exposure at RT. In order to check if heating to 400°C reconstructs the surface completely, a second series of measurements on a second MCBDD sample (MCBDD 2) was carried out and results are displayed as solid symbols in figure 7b. The sample was immersed at 400°C in the plasma and the decrease of the negative-ion yield was still observed. However, the yield went down by a factor of 2 instead of a factor of 3 seen previously, and the decrease was happening within ~ 20 min. In such a way, heating of MCBDD has hindered the creation of defects by the plasma exposure and has kept the surface in a state which is more favorable for negative-ion production. The red solid symbols show the continuation of experiment with MCBDD 2 sample after letting it cool down overnight in vacuum. One can notice that the

heated surface presents initially the same negative-ion yield as an unexposed sample, showing that the surface state at 400°C is close to an undisturbed surface state. For the second half of the experiment illustrated with solid red and green symbols in Figure 4, MCBDD 2 has acted as the sample MCBDD 1. Again, the heating to 400°C (solid green symbols) was performed in plasma with applied surface bias. The 15% of difference in the negative-ion yields between MCBDD 1 and MCBDD 2 in the same conditions are thought to be due to the experimental uncertainty comprising different durations of plasma exposure, uncertainty on the surface temperature, alignment of the normal to the sample surface with respect to the mass spectrometry axis, etc…

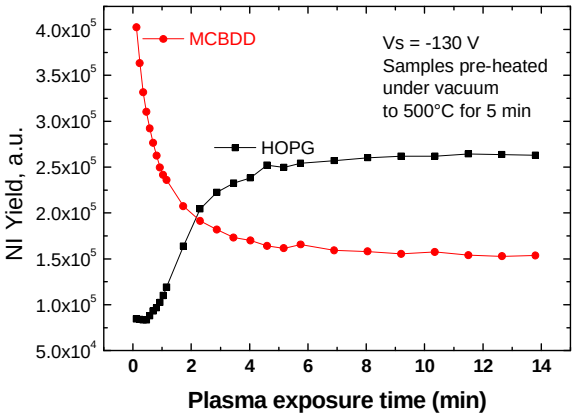

Figure 7a: Time evolution of Negative-ion (NI) yield for HOPG and MCBDD materials from the onset of the plasma. Samples have been heated under vacuum to 500°C during 5 minutes to release impurity before experiments started. D_2 plasma, 2 Pa, 20W, Vs = -130 V

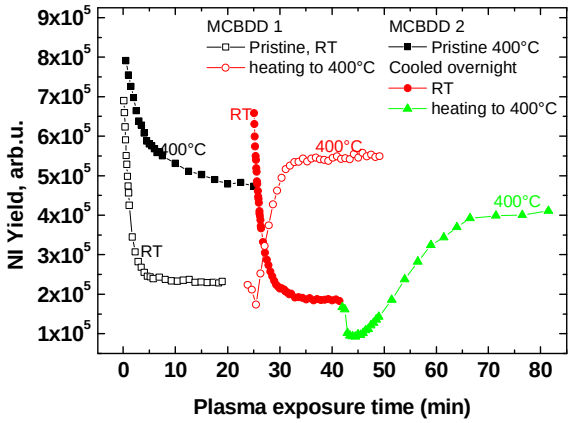

Figure 7b: Time evolution of NI yield on MCBDD at different surface temperatures under plasma exposure. Empty symbols correspond to MCBDD 1 sample and solid symbols to MCBDD 2. The color of symbols goes with the chronological order of the experiments: black, red, green. The surface temperature of the sample is indicated next to the curves with a corresponding color

All these results show that it would be interesting to work with less defective diamond layers. This can be achieved if the positive-ion energy is strongly reduced. Such a situation is relevant for fusion since in the ITER negative-ion source the plasma grid is biased few volts below the plasma potential. However, under our experimental conditions, the bias cannot be reduced too much since self-extraction of negative-ions is required. We found that working with a bias of -20 V is possible and that negative-ion are still efficiently extracted from the plasma. As the plasma potential is higher with this low bias, the positive ion energy is now 36 eV. H_3^+ ion is dominating the ion flux giving an impact energy of ~12 eV/nucleon. Let us note first that this energy is still large enough to create some defects. Indeed, we have followed negative-ion time evolution at V_s = -10 V corresponding to 9 eV/nucleon, and still observed a yield decrease identical as the one displayed on Figure 7a. The mass spectrometer nozzle is usually set at 0 V which is a requirement for the NIEDF modelling[97]. However, the mass spectrometer nozzle can be biased to positive value when modelling is not needed. We did bias it at + 10V and kept the sample surface at the ground potential leading to an impact energy of ~5 eV/nucleon. In this case we observed only a slight increase of

the negative-ion yield with time, no degradation has been evidenced. However, the signal was too low for a complete study, and a bias voltage of -20 V was chosen as representative of a situation where the positive ion flux does not induce too much defects. Figure 8 is presenting negative-ion yields obtained on different diamond layers versus surface temperature. Apart from the previous materials HOPG and MCBDD, two different Nano Crystalline Diamond layers have been used here, as well as a (100) Single Crystal Boron Doped Diamond (SCBDD). This 20 µm thick / 9 mm^2 area SCBDD was grown on a SUMITOMO HPHT diamond substrate. It was highly boron doped (10^{21} Boron atom/cm^3). NCD 1% and NCD 5% refers to the percentage of CO_2 used in the gas mixture during the deposition process. The two different layers have very similar Raman signature and differ by their grain size; few tens of nm and around 200 nm, see SEM pictures on figure 6).

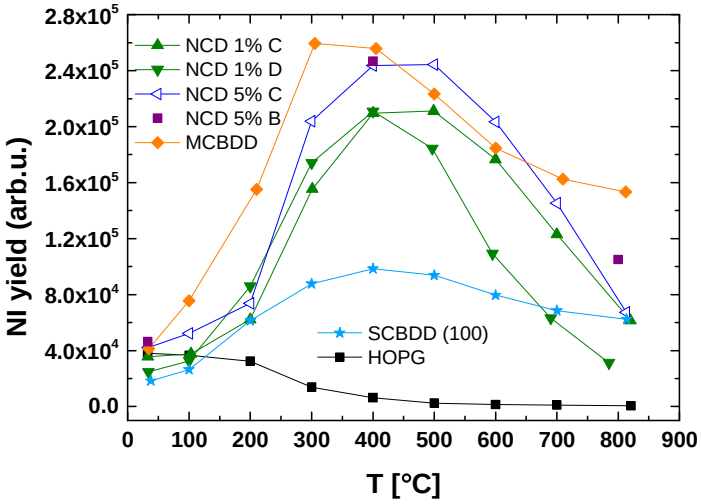

Figure 8: NI yield dependence on the surface temperature for HOPG, MCBDD, NCD 1%, NCD 5% and SCD (100). All diamond materials have been synthesized at LSPM laboratory (Paris 13 University). Label B, C and D refers to different samples of the same material. D_2 RF plasma, 20W, 2 Pa, V_s = - 20V.

First of all, figure 8 demonstrates the same global behavior of negative-ion yield versus surface temperature that is observed at higher positive ion energy. The yield is decreasing for HOPG while it is increasing for all diamond layers up to a maximum around 400 - 500°C after which it decreases. Again, we can assume that the increase of surface temperature favors the surface reconstruction and the recovery of pristine diamond electronic properties. Second, one can observe some dispersion in NCD measurements. The same material (NCD 1%) is giving two different negative-ion yields at high temperature even if both samples come from the same original layer that has been cut in parts. We have observed that NCD layers can handle several heating cycles without degrading their yields. Let us note that NCD layers are deposited at much lower temperature than MCD samples (less than 400°C compared to 800°C for MCD layers[108]. Finally, we can observe a similar negative-ion yield behavior for (100) Boron Doped Single Crystal Diamond as for micro- and nanocrystalline layers. The yield is much lower but this is probably due to a reduced size of 3 mm by 3 mm for the (100) SCBDD sample which makes its installation on the sample holder and

its alignment with the mass spectrometer somewhat complicated. It might even be possible that part of the signal measured for SCBDD comes from the molybdenum sample holder instead of the diamond layer explaining the low signal recorded.

From all the measurements presented here it is not possible to observe a clear influence of the crystalline structure of the diamond layer on the negative-ion yield. Most often the MCBDD or MCD samples produce a slightly higher yield than other materials but overall, a similar behavior is observed. NCD layers are interesting since they can be easily deposited on large surfaces at relatively low-temperature and could be maybe regenerated *in-situ*. However, they are expected to exhibit lower resistance to plasma exposure than microcrystalline layers because of their higher sp2 phase content[109,110]. The main purpose of the present study is not to choose between MCD or NCD, but rather to demonstrate if the electronic properties of diamond, in particular the negative-electron affinity, influence negative-ion yields, in order to go towards negative-ion yield optimization by tuning and designing the best material. We have shown that the less defective the diamond surface is, the higher the negative-ion yield is. Therefore, it seems that diamond electronic properties are relevant for negative-ion surface production, a suggestion supported by the next paragraph.

As seen before, MCD material cannot be DC biased when exposed to plasma at low temperature since the layer is insulating. In order to study insulating materials, we have developed a pulsed-DC bias scheme similar to the one described in [111] and [112] for the sputtering of insulating films or for the measurement of the positive ion flux at plasma wall. The detailed method will be described in a forthcoming paper. The principle is to apply to the insulating sample a short negative DC bias. As the sample is initially not charged, the applied bias appears on the surface. Positive ions from the plasma are attracted to the sample surface decreasing the surface bias. The decrease rate of the surface bias, in Volts/seconds is given by the ratio between the ion saturation current at the sample and the sample capacitance. Under our experimental conditions the ion saturation current never exceeds 100 $\mu A/cm^2$ and the diamond layer capacitance is on the order of 1 nF corresponding to 1 cm^2 sample and 5 µm thickness. This gives a surface bias decrease rate on the order of 0.1 V/µs. If the measurement is fast enough, the surface bias is almost constant during the measurement. The time resolution of the mass spectrometer being 2 µs, the measurement can be performed at almost constant bias. It allows studying insulating materials with the tools developed for conductive materials, same extraction, same modelling… Finally, when the bias is switched off, the electrons come to the surface to unload it before the next pulse starts.

The method has been applied to HOPG first for comparison with DC bias. Interestingly, HOPG has demonstrated higher yield under pulsed-DC bias that under DC bias conditions (figure 5). The analysis made with the model presented previously showed that under pulsed bias conditions the HOPG surface is more hydrogenated leading to an important amount of NI created by sputtering. A temperature scan has then been performed for HOPG and MCD materials at pulsed bias conditions given by ; -130 V, 2 Pa, D_2, 20 W, 15 µs pulse, 10 kHz repetition frequency. The result is shown on figure 5 which show that measurements on MCD have been successfully extended to low temperatures. The global behavior with temperature is similar to the DC bias mode: the yield is decreasing on HOPG when temperature is increased and the yield presents a maximum around 400°C for diamond material. However, the yield is increased by a factor 2 to 5 compared to

MCBDD in DC bias mode. If compared to HOPG at room temperature, the yield on MCD is almost one order of magnitude higher in pulsed mode at 400°C.

In the pulsed-DC bias scheme, the positive-ion bombardment only occurs during a short period of time. It is suggested that the increase of NI yield under pulsed bias conditions is the consequence of a less degraded surface with properties closer to a pristine diamond one. This is consistent with the previous studies demonstrating that surface defects tend to decrease the negative-ion yield. Also, as the surface is not conductive, some electrons coming from the plasma when the bias is off, might be trapped in defects in the band gap and might contribute to negative-ion surface production when the bias is ON. The identification of the exact electron-capture mechanism by incoming hydrogen ions still requires further investigation; it will be essential to optimize surface production on diamond or on any other material. It should be noted that the overall efficiency of pulsed bias mode is limited by the duty cycle which is here 15%. Nonetheless results show that diamond electronic properties are promising for the negative-ion surface production and that there is still room for optimization of negative-ion yield on these diamond layers.

Conclusion

The present papers deals with H^-/D^- negative-ion surface production in low-pressure H_2/D_2 plasmas. Different diamond materials ranging from nanocrystalline to single crystal layers, either doped with boron or intrinsic have been investigated and compared with HOPG. Measurements were performed in DC or pulsed bias conditions as a function of surface temperature. Boron doping eliminates the charging problem and was found to have no influence on negative-ion surface production. As to the crystalline structure, we have not been able to observe a clear effect, however we emphasized that the creation of defect on diamond surface by positive ion bombardment reduces the negative-ion surface production. We concluded that, compared with HOPG, the electronic properties of diamond, among which the negative electron-affinity, are probably responsible for the observed increase of the negative-ion surface production.

Acknowledgments

This work was carried out within the framework of the French Research Federation for Fusion Studies (FR-FCM) and the EUROfusion Consortium and has received funding from the Euratom research and training programme 2014-2018 under grant agreement No 633053. The views and opinions expressed herein do not necessarily reflect those of the European Commission. Financial support was received from the French Research Agency within the framework of the projects ITER-NIS 08-BLAN-0047, and H INDEX TRIPLED 13-BS09-0017. CGI (Commissariat à l'Investissement d'Avenir) is gratefully acknowledged for its financial support through Labex

SEAM (Science and Engineering for Advanced Materials and devices) ANR 11 LABX 086, IDEX 05 02

References

[1] Bacal M and Wada M 2015 Negative hydrogen ion production mechanisms *Applied Physics Reviews* 2 021305
[2] Béchu S, Soum-Glaude A, Bès A, Lacoste A, Svarnas P, Aleiferis S, Ivanov A A and Bacal M 2013 Multi-dipolar microwave plasmas and their application to negative ion production Physics of Plasmas 20 101601
[3] J. Komppula, O. Tarvainen, S. Lätti, T. Kalvas, H. Koivisto, V. Toivanen and P. Myllyperkiö (2013) VUV-diagnostics of a filament-driven arc discharge H− ion source *AIP Conference Proceedings*, 1515, 66-73
[4] J Peters, AIP, 1st international symposium on negative ions, beams and sources, Aix-en-Provence (France) (2009 DOI: 10.1063/1.3112518
[5] J Peters, The NEW DESY RF-Driven Multicusp H- Ion Source, 1st international symposium on negative ions, beams and sources, Aix-en-Provence (France), 9-12 Sep 2008, DOI: 10.1063/1.3112510AIP Conference Proceedings (2009) 1097(1)
[6] Fantz U, Franzen P and Wünderlich D 2012 Development of negative hydrogen ion sources for fusion: experiments and modelling *Chem. Phys.* **398** 7–16
[7] Schiesko L, McNeely P, Fantz U, Franzen P and NNBI Team 2011 Caesium influence on plasma parameters and source performance during conditioning of the prototype ITER neutral beam injector negative ion source *Plasma Physics and Controlled Fusion* 53 085029
[8] Ueno A *et al* 2010 Interesting experimental results in japan proton accelerator research complex H ion-source development (invited) *Rev. Sci. Instrum.* **81** 02A720
[9] Moehs D P, Peters J and Sherman J 2005 Negative hydrogen ion sources for accelerators *IEEE Trans. Plasma Sci.* **33** 1786–98
[10] Lettry J, Aguglia D, Andersson P, Bertolo S, Butterworth A, Coutron Y, Dallocchio A, Chaudet E, Gil-Flores J, Guida R, Hansen J, Hatayama A, Koszar I, Mahner E, Mastrostefano C, Mathot S, Mattei S, Midttun Ø, Moyret P, Nisbet D, Nishida K, O'Neil M, Ohta M, Paoluzzi M, Pasquino C, Pereira H, Rochez J, Alvarez J S, Arias J S, Scrivens R, Shibata T, Steyaert D, Thaus N and Yamamoto T 2014 Status and operation of the Linac4 ion source prototypesa) *Review of Scientific Instruments* 85 02B122
[11] Welton R.F. Aleksandrov A.V., Dudnikov V.G., Han B.X.1, Kang Y., Murray S.N., Pennisi T.R., Piller C., Santana M., Stockli M.P., Review of Scientific Instruments 2016, vol.87, no.2, 02B146
[12] Yoned M et al 2004 Nucl. Instrum. Methods Phys. Res. B 223–224 116–23
[13] Alton G D 1994 High-intensity, heavy negative ion sources based on the sputter principle Review of scientific instruments 65 1141–1147

[14] Aanesland A, Rafalskyi D, Bredin J, Grondein P, Oudini N, Chabert P, Levko D, Garrigues L and Hagelaar G 2015 The PEGASES Gridded Ion-Ion Thruster Performance and Predictions *IEEE Transactions on Plasma Science* **43** 321–6
[15] Lafleur T, Rafalskyi D and Aanesland A 2015 Alternate extraction and acceleration of positive and negative ions from a gridded plasma source *Plasma Sources Sci. Technol.* 24 015005
[16] D. Renaud, D. Gerst, S. Mazouffre and A. Aanesland 2015 E × B probe measurements in molecular and electronegative plasmas *Rev. Sci. Instrum.* 86, 123507
[17] Samukawa S, Sakamoto K and Ichiki K 2001 High-efficiency low energy neutral beam generation using negative ions in pulsed plasma *Japan. J. Appl.Phys. Part 2* **40** L997–9
[18] Thomas C, Tamura Y, Okada T, Higo A and Samukawa S 2014 Estimation of activation energy and surface reaction mechanism of chlorine neutral beam etching of GaAs for nanostructure fabrication *Journal of Physics D: Applied Physics* 47 275201
[19] Thomas C, Tamura Y, Syazwan M E, Higo A and Samukawa S 2014 Oxidation states of GaAs surface and their effects on neutral beam etching during nanopillar fabrication *J. Phys. D-Appl. Phys.* 47 215203
[20] Draghici M and Stamate E 2010 Properties and etching rates of negative ions in inductively coupled plasmas and dc discharges produced in Ar/SF6 *J. Appl. Phys.* **107** 123304
[21] Vozniy O V and Yeom G Y 2009 High-energy negative ion beam obtained from pulsed inductively coupled plasma for charge-free etching process *Appl. Phys. Lett.* **94** 231502
[22] D Marinov, Z el Otell, M D Bowden and N St J Braithwaite 2015 Extraction and neutralization of positive and negative ions from a pulsed electronegative inductively coupled plasma *Plasma Sources Science and Technology*, Volume 24, Number 6
[23] Romanelli F. 2012 A roadmap to the realization of fusion energy Fusion Electricity *European Fusion Development Agreement (EFDA)* ISBN 978-3-00-040720-8
[24] Franke T. *et al* 2015 *Fusion Eng. Des.* **96–97** 468–72
[25] U. Fantz, P. Franzen, and D. W€underlich, “Development of negative hydrogen ion sources for fusion: Experiments and modeling,” Chem. Phys. 398, 7–16 (2012).
[26] P. Franzen and U. Fantz, Fusion Eng. Des. 89, 2594 (2014).
[27] Babkina T, Gans T and Czarnetzki U 2005 Energy analysis of hyperthermal hydrogen atoms generated through surface neutralisation of ions *Europhys. Lett.***72** 235–41
[28] Schiesko L *et al* 2008 H-production on a graphite surface in a hydrogen plasma *Plasma Sources Sci. Technol.* **17** 035023
[29] Britun N, Minea T, Konstantinidis S and Snyders R 2014 Plasma diagnostics for understanding the plasma–surface interaction in HiPIMS discharges: a review Journal of Physics D: Applied Physics 47 224001
[30] Mahieu S and Depla D 2007 Correlation between electron and negative O[sup −] ion emission during reactive sputtering of oxides *Applied Physics Letters* 90 121117
[31] Toyoda H, Goto K, Ishijima T, Morita T, Ohshima N and Kinoshita K 2009 Fine Structure of O - Kinetic Energy Distribution in RF Plasma and Its Formation Mechanism *Applied Physics Express* 2 126001
[32] Ishijima T, Goto K, Ohshima N, Kinoshita K and Toyoda H 2009 Spatial Variation of Negative Oxygen Ion Energy Distribution in RF Magnetron Plasma with Oxide Target Japanese J*ournal of Applied Physics* 48 116004
[33] Andersson J M, Wallin E, Münger E P and Helmersson U 2006 Energy distributions of positive and negative ions during magnetron sputtering of an Al target in Ar⁄O[sub 2] mixtures *Journal of Applied Physics* 100 33305
[34] Mahieu S, Leroy W P, Van Aeken K and Depla D 2009 Modeling the flux of high energy negative ions during reactive magnetron sputtering *Journal of Applied Physics* 106 093302
[35] Norihiro Ito, Nobuto Oka, Yasusi Sato, and Yuzo Shigesato 2010 Effects of Energetic Ion Bombardment on Structural and Electrical Properties of Al-Doped ZnO Films Deposited by RF-Superimposed DC Magnetron Sputtering *Jpn. J. Appl. Phys. 49* 071103
[36] Britun N, Minea T, Konstantinidis S and Snyders R 2014 Plasma diagnostics for understanding the plasma–surface interaction in HiPIMS discharges: a review *Journal of Physics D: Applied Physics* 47 224001
[37] Hayashi T. et al Japanese Journal of Applied Physics, 50, pp. 08KB01-08KB01-4 (2011)
[37] Ito, N; Oka, N ; Sato, Y; Shigesato, Y; Jpn J. Appl. Phys. 49 071103 (2010)

[38] Jens-Peter Krumme, Ron A. A. Hack., Ivo J. M. M. Raaijmakers, J. Appl. Phys. 70 (1991) 6743
[39] Stanislav Mráz and Jochen M. Schneider, J. Appl. Phys. 100, 023503 (2006)
[40] H. Oomori, T. Kasuya, and M. Wada, Y. Horino and N. Tsubouchi, Rev. Sci. Instrum., 71 (2000) 1123
[41] Kikuo Tominaga and Takuya Kikuma, J. Vac. Sci. Technol. A 19.4., (2001) 1582
[42] Hiroki Matsui, Hirotaka Toyoda, and Hideo Sugai, J. Vac. Sci. Technol. A 23.4., (2005) 671

[43] N. Tsukamoto, D. Watanabe, M. Saito, Y. Sato, N. Oka, Y.Shigesato, J. Vac. Sci. Tech. A 28, 846 (2010)
[44] Th. Welzel, S. Naumov, and K. Ellmer, J. Appl. Phys. 109, 073302 (2011)
[45] F. Richter, T. Welzel, R. Kleinhempel, et al, Surface & Coatings Technology 204 (2009) 845–849
[46] M. Zeuner, H. Neumann, J. Zalman and H. Biederman, J. Appl. Phys., Vol. 83, No. 10, (1998) 5084
[47] R. Wendt and K. Ellmer, Surface and Coatings Technology 93 (1997) 27-31
[48] Wyputta F, Zimny R, Winter H, H- formation in grazing collisions of fast protons with an Al(111) surface, NIMB 58 (1991) 379
[49] H. Verbeek, W. Eckstein, R.S. Bhattacharya, Surface Science 95 (1980) 380-390
[50] P. Roncin, A. G. Borisov, H. Khemliche, and A. Momeni, A. Mertens and H. Winter, Phys. Rev. Lett. 89, 043201 (2002)
[51] A.G. Borisov, V. Sidis, P. Roncin, A. Momeni, H. Khemliche, A. Mertens and H. Winter; Physical review B. Condensed matter and materials physics, (2003) **67**, pp. 115403.1-115403.13
[52] M. Maazouz, L. Guillemot, V.A. Esaulov, D.J. O'Connor Surface Science 398 (1998) 49-59
[53] M. Maazouz, A. G. Borisov, V. A. Esaulov, et al, Phys. Rev. B **55**, 13 869 (1997)
[54] M. A. Gleeson, M. Kropholler and A. W. Kleyn, Appl. Phys. Lett., Vol. 77, No. 8, 21 (2000)
[55] J.A. Scheer, M. Wieser, P. Wurz, P. Bochsler, E. Hertzberg, S.A. Fuselier, F.A. Koeck, R.J. Nemanich, M. Schleberger, Nuclear Instruments and Methods in Physics Research B 230 (2005) 330–339
[56] R. Souda, E. Asari, H. Kawanowa, T. Suzuki, S. Otani, Surface Science 421 (1999) 89–99
[57] S. G. Walton, R. L. Champion, Yicheng Wang, J. Appl. Phys., Vol. 84, No. 3, 1 1998
[58] A G Borisov and V A Esaulov 2000 J. Phys.: Condens. Matter 12 R177
[59] Borisov A G, Teillet-Billy D and Gauyacq J P 1992 H- formation by electron capture in hydrogen-Al (111) collisions: perturbative and nonperturbative approaches Surface science 278 99–110
[60] D. Teillet-Billy and J.P. Gauyacq Resonant electron capture in atom metal collisions: H-Al(111) Surface science 269/270 (1992) 162
[61] Los and Geerlings, Phys.Rep. 190 (1990) 133
[62] Michaelson H B 1977 The work function of the elements and its periodicity Journal of Applied Physics 48 4729
[63] C.A. Papageorgopolous, J. Chen, Cs and H2 adsorption on W(100), J. Phys. C: Solid State Phys. 6 (1973) L279
[64] Fehrs et al, Surf Science 24 (1971) 309
[65] Friedl, R.; Fantz, U., Temperature Dependence of the Work Function of Caesiated Materials under Ion Source Conditions, AIP Conference Proceedings Volume: 1655 020004 Published2015
[66] Gutser R, Wimmer C and Fantz U 2011 Work function measurements during plasma exposition at conditions relevant in negative ion sources for the ITER neutral beam injection Review of Scientific Instruments 82 23506
[67] Fröschle M, Riedl R, Falter H, Gutser R and Fantz U 2009 Recent developments at IPP on evaporation and control of caesium in negative ion sources Fusion Engineering and Design 84 788–92
[68] A. G. Borisov and V. Sidis, Phys. Rev. Lett. 77, 1893–1896 (1996)
[69] Blauth D and Winter H 2011 Negative ions, energy loss, and electron emission during grazing scattering of fast H and He atoms from a clean and oxidized NiAl(110) surface Nuclear Instruments and Methods in Physics Research Section B: Beam Interactions with Materials and Atoms 269 1175–8
[70] Winter H, Mertens A, Lederer S, Auth C, Aumayr F and Winter H 2003 Electronic processes during impact of fast hydrogen atoms on a LiF() surface Nuclear Instruments and Methods in Physics Research Section B: Beam Interactions with Materials and Atoms 212 45–50
[71] V. Dudnikov, SU patent application C1.H013/04, No. 411542(10 March 1972)
[72] Dudnikov V, Rev. Sci. Instrum. **73** (2002) 993
[73] Dudnikov V 2012 Forty years of surface plasma source development Review of Scientific Instruments 8302A708
[74] Heeren R M A et al 1994 Angular and energy distributions of surface produced H−and D−ions in a barium surface conversion source *J. Appl. Phys.* 75 4340
[75] C. F. A. van Os, W. B. Kunkel, C. Leguijt, and J. Los, J. Appl. Phys. 70, 2575 (1991)
[76] C. F. A. van Os, P. W. van Amersfoort, and J. Los, J. Appl. Phys. 64, 3863 (1988)
[77] R.M.A. Heeren, D. Ciric, S . Yagura, H.J . Hopman and A.W. Kleyn, Nuclear Instruments and Methods in Physics Research B69 (1992) 389-402
[78] K. N. Leung, S. R. Walther, and W. B. Kunkel, Phys. Rev. Lett. 62 (1989) 764
[79] P. G. Steen and W. G. Graham, Appl. Phys. Lett. **75** (1999) 2738
[80] Kurutz, U.; Fantz, U., Investigations on Caesium-free Alternatives for H- Formation at Ion Source Relevant Parameters, AIP Conference Proceedings Volume: 1655, 020005 (2015)

[81] L. Schiesko, G. Cartry, C. Hopf, T. Höschen, G. Meisl, O. Encke, B. Heinemann, K. Achkasov, P. Amsalem, and U. Fantz, First experiments with Cs doped Mo as surface converter for negative hydrogen ion Sources, J. Appl. Phys. 118, 073303 (2015)
[82] L. Schiesko, G. Cartry, C. Hopf, T. Höschen, G. Meisl, O. Encke, P. Franzen, B. Heinemann, K. Achkasov, C. Hopf and U. Fantz, Cs-Doped Mo as Surface Converter for H- / D- Generation in Negative Ion Sources: First Steps and Proof of Principle, AIP CONFERENCE PROCEEDINGS, AIP Conf. Proc. 1655, 010001 (2015)
[83] Fantz U, Franzen P, Kraus W, Berger M, Christ-Koch S, Falter H, Fröschle M, Gutser R, Heinemann B, Martens C, McNeely P, Riedl R, Speth E, Stäbler A and Wünderlich D 2009 Physical performance analysis and progress of the development of the negative ion RF source for the ITER NBI system Nuclear Fusion 49 125007
[84] Y. Xiang, PhD thesis, Université Paris-Sud (2012), *https://tel.archives-ouvertes.fr/tel-00863479/document*
[85] J. Lienemann, D. Blauth, S. Wethekam, M. Busch, H. Winter, P. Wurz, S.A. Fuselier, E. Hertzberg, Nuclear Instruments and Methods in Physics Research B269, 915 (2011)
[86] M.A. Gleeson, A.W. Kleyn, Nuclear Instruments and Methods in Physics Research B 157 (1999) 48-54
[87] Kumar P, Ahmad A, Pardanaud C, Carrère M, Layet J M, Cartry G, Silva F, Gicquel A and Engeln R 2011 Enhanced negative ion yields on diamond surfaces at elevated temperatures Journal of Physics D: Applied Physics 44 372002
[88] S. Zuo, M. K. Yaran, T. A. Grotjohn, D. K. Reinhard, J. Asmussen (2008) "Investigation of diamond deposition uniformity and quality for freestanding film and substrate applications" Diam.&Relat. Mat. 17, p. 300
[89] T. Tachibana, Y. Ando, A. Watanabe, Y. Nishibayashi, K. Kobashi, T. Hirao and K. Oura (2001) "Diamond films grown by a 60-kW microwave plasma chemical vapor deposition system" Diam. & Relat. Mat. 10, p. 1569
[90] O. A. Williams, M. Daenen, J. D'Haen, K. Haenen, J. Maes, V. V. Moshchalkov, M. Nesladek and D. M. Gruen (2006) "Comparison of the growth and properties of ultrananocrystalline diamond and nanocrystalline diamond" Diam. & Relat. Mat. 15, p. 654
[91] P. W. May and Y. A. Mankelevich (2006) "Experiment and modeling of the deposition of ultrananocrystalline diamond films using hot filament chemical vapor deposition and Ar/CH[sub 4]/H[sub 2] gas mixtures: A generalized mechanism for ultrananocrystalline diamond growth" J. Appl. Phys. 100, p. 024301
[92] F. Silva, F. Benedic, P. Bruno and A. Gicquel (2005) "Formation of <110> texture during nanocrystalline diamond growth: an X-ray diffraction study" Diam. & Relat. Mat. 14, p. 398
[93] Diederich L, Küttel O M, Aebi P and Schlapbach L 1998 Electron affinity and work function of differently oriented and doped diamond surfaces determined by photoelectron spectroscopy Surface science 418 219–239
[94] Diederich L, Küttel O M, Aebi P and Schlapbach L 1999 Electron emission and NEA from differently terminated, doped and oriented diamond surfaces Diamond and related materials 8 743–747
[95] Cui, J. B.; Stammler, M.; Ristein, J.; Ley, L. Journal of Applied Physics. 88 (2000) p3667
[96] Yater J and Shih A 2000 J. Appl. Phys. 87 8103
[97] Ahmad A, Dubois J, Pasquet T, Carrère M, Layet J M, Faure J B, Cartry G, Kumar P, Minéa T, Mochalskyy S and Simonin A 2013 Negative-ion surface production in hydrogen plasmas: modeling of negative-ion energy distribution functions and comparison with experiments Plasma Sources Science and Technology 22 25006
[98] Dubois J P J, Achkasov K, Kogut D, Ahmad A, Layet J M, Simonin A and Cartry G 2016 Negative-ion surface production in hydrogen plasmas: Determination of the negative-ion energy and angle distribution function using mass spectrometry Journal of Applied Physics 119 193301
[99] J. F. Ziegler, J. P. Biersack, and M. D. Ziegler, SRIM—The Stopping and Range of Ions in Matter (SRIM Co., 2008), ISBN 0-9654207-1-X.
[100] Schiesko L, Carrère M, Layet J-M and Cartry G 2009 Negative ion surface production through sputtering in hydrogen plasma Applied Physics Letters 95 191502
[101] Schiesko L, Carrère M, Layet J-M and Cartry G 2010 A comparative study of H − and D − production on graphite surfaces in H 2 and D 2 plasmas Plasma Sources Science and Technology 19 45016
[102] Cartry G, Schiesko L, Hopf C, Ahmad A, Carrère M, Layet J M, Kumar P and Engeln R 2012 Production of negative ions on graphite surface in H2/D2 plasmas: Experiments and srim calculations Physics of Plasmas 19 63503
[103] Submitted to Plasma Sources Science and Technology
[104] Ahmad A, Pardanaud C, Carrère M, Layet J-M, Gicquel A, Kumar P, Eon D, Jaoul C, Engeln R and Cartry G 2014 Negative-ion production on carbon materials in hydrogen plasma: influence of the carbon hybridization state and the hydrogen content on H − yield Journal of Physics D: Applied Physics 47 85201
[105] Simonin A, Achard J, Achkasov K, Bechu S, Baudouin C, Baulaigue O, Blondel C, Boeuf J P, Bresteau D, Cartry G, Chaibi W, Drag C, de Esch H P L, Fiorucci D, Fubiani G, Furno I, Futtersack R, Garibaldi P, Gicquel A, Grand C, Guittienne P, Hagelaar G, Howling A, Jacquier R, Kirkpatrick M J, Lemoine D, Lepetit B, Minea T, Odic E, Revel A, Soliman B A and Teste P 2015 R&D around a photoneutralizer-based NBI system (Siphore) in view of a DEMO Tokamak steady state fusion reactor Nuclear Fusion 55 123020

[106] Yamazaki Y, Ishikawa K, Mizuochi N and Yamasaki S 2006 Diamond Relat. Mater. 15 703–6
[107] Villalpando I, John P, Porro S andWilson J I B 2011 Hydrogen plasma etching of diamond films deposited on graphite Diamond Relat. Mater. 20 711–6
[108] Baudrillart, Benoit; Benedic, Fabien; Brinza, Ovidiu, Bieber, Thomas, Chaveau Thierry, Achard Jocelyn, Gicquel Alix *Microstructure and growth kinetics of nanocrystalline diamond films deposited in large area/low temperature distributed antenna array microwave-plasma reactor* PHYSICA STATUS SOLIDI A-APPLICATIONS AND MATERIALS SCIENCE Volume: 212 Issue: 11 Special Issue: SI Pages: 2611-2615 Published: NOV 2015
[109] Porro S, De Temmerman G, John P, Lisgo S, Villalpando I and Wilson J I B 2009 Effects in CVD diamond exposed to fusion plasmas phys. stat. sol. (a) 206 2028–32
[110] Porro S, Temmerman G D, Lisgo S, Rudakov D L, Litnovsky A, Petersson P, John P and Wilson J I B 2011 Diamond coatings exposure to fusion-relevant plasma conditions Journal of Nuclear Materials 415 S161–4
[111] Barnat E and Lu T-M 1999 Pulsed bias magnetron sputtering of thin films on insulators Journal of Vacuum Science & Technology A: Vacuum, Surfaces, and Films 17 3322
[112] Šamara V, Booth J-P, Marneffe J-F de, Milenin A P, Brouri M and Boullart W 2012 A dc-pulsed capacitively coupled planar Langmuir probe for plasma process diagnostics and monitoring Plasma Sources Science and Technology 21 65004